RSC Advances

PAPER

View Article Online
View Journal | View Issue

Cite this: *RSC Adv.*, 2018, **8**, 32423

Niobium phosphotungstates: excellent solid acid catalysts for the dehydration of fructose to 5-hydroxymethylfurfural under mild conditions†

Guo Qiu,[a] Xincheng Wang,[b] Chongpin Huang,*[a] Yingxia Li[a] and Biaohua Chen[a]

The efficient conversion of carbohydrates to 5-hydroxymethylfurfural (5-HMF) under mild conditions represents a very attractive and promising method of producing important building blocks. In this work, niobium phosphotungstates, with Nb/P molar ratios of 0.6, 1.0, 2.0 and 4.0 (NbPW-06, NbPW-1, NbPW-2, and NbPW-4, respectively) have been prepared by a facile, one-pot, alcohol-mediated thermal process and used for the direct conversion of fructose to 5-HMF. By adding a certain amount of Nb, the surface of the catalyst became enriched in P, and this enrichment was associated with the presence of surface P–OH groups that offered Brønsted acid sites that can activate superficial hydrogen species to facilitate 5-HMF generation. Pyridine-FTIR confirmed the presence of Brønsted and Lewis acid sites, which might play important roles in the dehydration of fructose to 5-HMF. Furthermore, polar aprotic solvents were well-suited for the conversion, and higher yields of 5-HMF were obtained in polar aprotic solvents than in nonpolar solvents. A 5-HMF yield of 96.7% with complete fructose consumption was obtained over NbPW-06 in DMSO at 80 °C after 90 min. In addition, NbPW-06 could be recycled several times without a significant decrease in the catalytic activity. A catalytic mechanism for this reaction was proposed. Moreover, this catalytic system can also be utilized for the dehydration of sucrose and inulin to 5-HMF in satisfactory yields. This study establishes an important platform for the further design of Nb-containing catalysts for the production of 5-HMF from carbohydrates under mild conditions.

Received 12th July 2018
Accepted 7th September 2018

DOI: 10.1039/c8ra05940c

rsc.li/rsc-advances

1. Introduction

With the rapid growth of the world economy, the high dependence on fossil fuels has caused serious environmental problems and requires groundbreaking improvements in clean technology that will take advantage of renewable energy sources.[1,2] Biomass represents an abundant and renewable carbon resource that can be transformed into liquid fuels and value-added chemicals. The catalytic conversion of biomass has been the subject of intense research efforts in recent years.[3–6] As a promising raw material with numerous industrial applications, carbohydrates have been employed in diverse areas of the food, chemistry, paper and pharmaceutical industries.[7] One of the key building blocks derived from carbohydrates is 5-hydroxymethylfurfural (5-HMF), which has been identified as one of the most important biomass-derived platform compounds and is widely utilized in the synthesis of various chemicals.[8–11]

A variety of catalysts, including both homogeneous and heterogeneous catalysts, have been employed for the conversion of fructose to obtain 5-HMF. Several homogeneous catalysts, such as mineral or organic acids,[12–14] Lewis acids,[15] inorganic salts,[16] and ionic liquids,[17–19] have been found to be effective for the synthesis of 5-HMF from fructose. However, the isolation of these catalysts from the reaction products and subsequent recovery are major impediments to their potential industrial application. Therefore, heterogeneous catalysts that can be separated from the products by filtration have been developed for the conversion of fructose to 5-HMF, for instance solid heteropolyacid $Cs_{2.5}H_{0.5}PW_{12}O_{40}$,[20] sulfated zirconia,[21] Fe_3O_4–SBA–SO_3H,[22] tungstated zirconia,[23] zirconium oxophosphate,[24] acidic resin,[25,26] and tin-beta zeolite,[27] metal–organic frameworks (MOFs),[28] covalent organic frameworks (COFs),[29] and nanostructured niobium oxide.[30] These catalysts are efficient and recyclable in the dehydration of fructose, and these findings have inspired further studies on heterogeneous catalysts.

Among heterogeneous catalysts, niobium compounds and related materials have recently attracted much attention as industrial catalysis due to their intrinsic acidity and redox properties.[31,32] For instance, high yields (86.2%) of 5-HMF were achieved with a Nb_2O_5-catalyzed conversion of fructose in DMSO after 2 h at 120 °C.[33] Sulfated mesoporous niobium oxide provided a higher yield of 5-HMF (up to 88%) and showed better

[a]State Key Laboratory of Chemical Resource Engineering, Beijing University of Chemical Technology, Beijing 100029, China. E-mail: huangcp@mail.buct.edu.cn; Fax: +86 10 6441 9619; Tel: +86 10 6441 2054

[b]Beijing Key Laboratory of Fuels Cleaning and Advanced Catalytic Emission Reduction Technology, Beijing Institute of Petrochemical Technology, Beijing 102617, China

† Electronic supplementary information (ESI) available. See DOI: 10.1039/c8ra05940c

recyclability than what was observed with commercial Nb_2O_5.[34] Xue *et al.* developed a novel Nb-containing catalyst by the reaction of niobium chloride and nitrilotris (methylenephosphonic acid), and that catalyst provided a 5-HMF yield of 85.6% from the dehydration of fructose in a DMA–NaBr mixture after 1.5 h.[11] However, niobium compounds catalyst existed problems such as complex preparation, higher reaction temperature and the existence of by-products. Therefore, these findings inspired us to develop a promising and readily prepared Nb-containing catalytic system for the conversion of fructose to 5-HMF under mild conditions (less than 100 °C) with high throughput.

Keggin-type heteropolyacids (HPAs) have well-defined structures with a central cation (heteroatoms: P, As, Si, Ge, B, *etc.*) surrounded by polyanions. They are protonic acids with strong Brønsted acidity,[35,36] and they have been widely utilized in many reactions.[37,38] In the conversion of biomass, their reactivity was attributed to their acidity, and their other properties vary significantly based on their structural characteristics and heteroatoms. Recently, Xiao *et al.* reported that $H_3PW_{12}O_{40}$ (HPW) and $H_4SiW_{12}O_{40}$ (HSiW) could convert fructose to 5-HMF with high selectivity (99%) in an ionic liquid solvent, 1-butyl-3-methyl imidazolium chloride, within 5 min at 80 °C.[39] However, the homogeneous HPA catalysts suffer from complicated separation and recycling procedures. Hence, there is great interest in the design of heterogeneous catalyst containing heteropolyanions for the production of 5-HMF from fructose. For example, $Cs_{2.5}H_{0.5}PW_{12}O_{40}$ with a Keggin cluster synthesized *via* Cs^+-mediated proton exchange can convert fructose to 5-HMF with a final selectivity of 94.7% in 60 min at 115 °C.[20] Fan *et al.* reported that a high yield of 5-HMF (77.7%) with a selectivity of 93.8% could be obtained from fructose after 60 min using $Ag_3PW_{12}O_{40}$ at 120 °C.[40] These achievements indicate that heteropolyanions are potential candidates for the catalytic conversion of fructose to 5-HMF.

In the present study, solid niobium phosphotungstate catalysts were prepared by a simple alcohol-mediated thermal approach, and the effects of the amount of Nb on the acidity and activity were investigated. The main reaction parameters when using different heterogeneous catalysts have been studied. The as-prepared NbPW materials were excellent and efficient heterogeneous catalyst for the dehydration of fructose to 5-HMF using DMSO as the solvent under mild conditions. This method also provides an alternative for the production of 5-HMF in high yields under mild conditions, which makes it an important platform for the development of Nb-containing catalyst for the conversion of carbohydrates to 5-HMF.

2. Experimental section

2.1 Materials and instrumentation

5-HMF (98%), D-fructose (99%), sucrose (99%) and inulin (99%) were purchased from the Aladdin Chemistry Reagent Company (Shanghai, China). Methanol, ethanol, *n*-butanol (butan-1-ol), *sec*-butanol (butan-2-ol), dimethyl sulfoxide (DMSO), dimethylacetamide (DMA), dimethylformamide (DMF), methyl isobutyl ketone (MIBK), acetone and *N*-methyl pyrrolidone (NMP) were purchased from J&K Scientific Ltd. (Beijing, China). HPW, phosphomolybdic acid (HPMo), HSiW, niobium(v) chloride, niobium(v) oxide, cesium nitrate, chromium(iii) chloride, and stannic chloride were purchased from the Alfa Aesar Company (Shanghai, China). All reagents were used as received without further purification.

To elucidate the structures of the niobium phosphotungstate materials, powder X-ray diffraction (PXRD) (D8FOCUS, Bruker), X-ray photoelectron spectroscopy (XPS) (ESCALAB-250, ThermoFisher Scientific), Fourier transform infrared spectroscopy (FTIR) (TENSOR 27, Bruker), transmission electron microscopy (TEM) (JEM-3010, JEOL), and solid-state ^{31}P magic angle spinning (MAS) nuclear magnetic resonance (NMR) spectroscopy (AV300, Bruker) were employed. The coordination of niobium and phosphorus and the structure of the tungsten species were examined by UV-vis diffuse reflectance spectroscopy (DRS) with a Shimadzu UV-3600 spectrophotometer, and $BaSO_4$ was utilized as a reference. The type of acid and its strength can be clearly differentiated by pyridine-FTIR spectroscopy. The total number of acid sites on the niobium phosphotungstate materials was determined by temperature-programmed desorption of ammonia (NH_3-TPD) (OmniStar, MS200). Thermogravimetric analysis (TGA) was carried out in the range of 50–500 °C using a Perkin-Elmer TGA 7 thermal analyzer.

2.2 Catalysts preparation

NbPW was prepared by an alcohol-mediated heating method. In a typical synthesis, a certain amount of $H_3PW_{12}O_{40}$ was dissolved in ethanol (90 mL), and the mixture was stirred for 2 h at 40 °C. A certain amount of $NbCl_5$ was dissolved in ethanol (50 mL) and subjected to ultrasonic treatment for 10 min. The $NbCl_5$ solution was then added dropwise to the stirred $H_3PW_{12}O_{40}$ solution, and the resultant mixture was then stirred for another 12 h. The catalyst was obtained after rotary evaporation at 50 °C and drying at 120 °C overnight. Finally, the catalyst was calcined at 300 °C in static air for 3 h. These as-prepared materials were designated NbPW-06, NbPW-1, NbPW-2, and NbPW-4 based on the mole ratio of $NbCl_5$ to $H_3PW_{12}O_{40}$. Different types of HPW-based metal catalysts and Nb-based heteropolyacid salt catalysts were synthesized using hydrothermal methods and an alcohol-mediated heating method, respectively.

2.3 General procedure for the conversion of carbohydrates to 5-HMF

In the dehydration reaction, a sealed tube with a capacity of 15 mL was charged with certain amounts of carbohydrates, catalyst, and solvent, placed in a temperature-controlled oil bath, and stirred at a constant rate of 300 rpm using an internal stirrer. The temperature was monitored by a thermocouple in contact with the solution. After the reaction, the mixture was immediately quenched by submersion in an ice water bath, filtered through a 0.2 μm syringe filter, and then decanted into a volumetric flask using water as a diluent prior to analysis.

The product of the reaction was analyzed by high-performance liquid chromatography (HPLC) using a system

equipped with a UV detector and a C18 column. A mixture of deionized water/methanol (60/40 v/v) was used as the mobile phase with a flow rate of 1 mL min^{-1}. The residual carbohydrates were analyzed by HPLC with a Shodex IR detector and a Hypersil APS-2 column. The column temperature was set at 35 °C, and water was used as the mobile phase at a flow rate of 0.2 mL min^{-1}.

3. Results and discussion

3.1 Characterization of the niobium phosphotungstate

The XRD patterns of the niobium phosphotungstate samples (NbPW-06, NbPW-1, NbPW-2, and NbPW-4) are displayed in Fig. 1 and S7,† and NbPW-06 and NbPW-1 showed X-ray diffractograms typical of the body-centered cubic secondary structure of Keggin anions, compared to HPW. The patterns showed characteristic diffraction peaks at 10.38°, 25.38°, and 34.68°, which were very similar to those of HPW. Notably, a significant reduction in the intensity of the characteristic diffraction peaks and a slight upward shift were observed with increasing Nb content. The decrease in the value of X-ray diffraction peaks is likely due to the niobium insertion into the secondary Keggin structure.[35] With increasing Nb content, the characteristic peaks of the HPW in the XRD patterns of NbPW-2- and -4 become less obvious, which could be attributed to the existence of some changes in the structure of the NbPW-2- and -4. Only one broad diffraction peak was observed for NbPW-2 and NbPW-4, indicating they were amorphous.[11] The intensities of the characteristic diffraction peaks of the calcined catalysts were slightly lower than those of the as-synthesized catalysts.

The FTIR spectra of both the as-synthesized and the calcined NbPW are shown in Fig. 2. The Keggin structure is general believed to be an edge-sharing octahedral that contains a PO_4 tetrahedron surrounded by four W_3O_9 groups.[41] Obviously, the spectra show sharp bands at 1080 cm^{-1} that correspond to asymmetric P–O stretching vibrations, while the band at 596 cm^{-1} can be attributed to P–O bending vibrations. The bands at 984 cm^{-1}, 885 cm^{-1}, and 810 cm^{-1} were assigned to W–O_d (terminal oxygen), W–O_c–W (inter-bridge oxygen, between corner-sharing WO_6 octahedra), and W–O_e–W (intra-bridge oxygen, between edge-sharing WO_6 octahedra), respectively.[36] The Keggin structure of HPW was maintained in the NbPW materials.

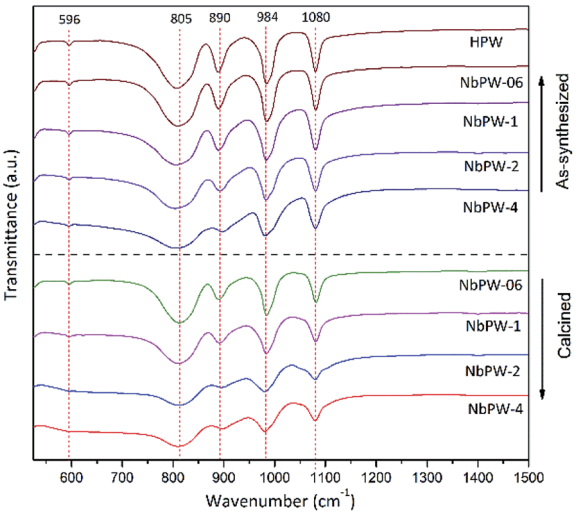

Fig. 2 FTIR spectra of NbPW.

The solid-state ^{31}P MAS NMR spectra of NbPW-06 were shown in Fig. 3(a). The sharp resonance at −16.00 ppm was assigned to the chemical shift (δp) of phosphorus, and the peak showed an obvious shift to more negative values compared to the corresponding signal from HPW ($\delta p = -15.0$ ppm);[42] this shift indicated the progressive deprotonation of phosphorus atoms is common during the synthesis.[43] A resonance peak at −12.23 ppm was observed in the spectrum of the calcined NbPW-06, and it may be a result of the interaction between the Keggin tungstophosphate anion and the Nb^{5+} ion after calcination. Fig. 3(b) presents the UV-vis DRS spectra of NbPW and HPW. The spectra of both the NbPW materials and HPW show two absorption bands, and the peak at 251 nm may be attributable to the oxygen–metal charge transfer that occurs at the tungstophosphate anion $[PW_{12}O_{40}]^{3-}$, and the peak at 320 nm corresponds to the formation of small clusters of bulk WO_3 particles, indicating the presence of octahedral coordination in

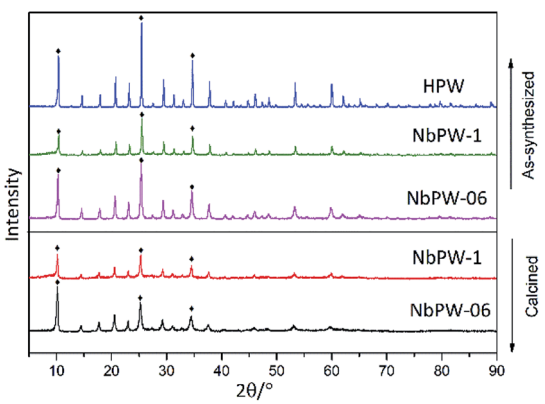

Fig. 1 The X-ray diffraction patterns of HPW, NbPW-06, and NbPW-1.

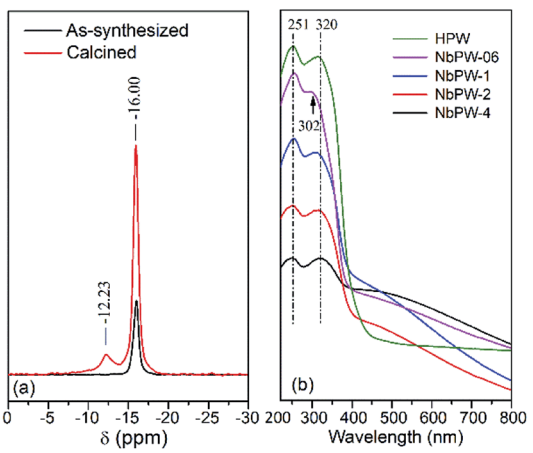

Fig. 3 (a) ^{31}P NMR spectra of NbPW-06. (b) UV-vis DRS spectra of NbPW.

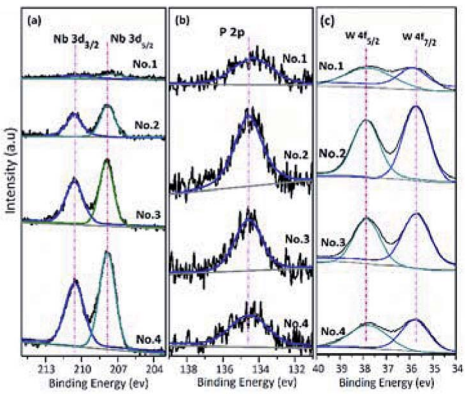

Fig. 4 Nb 3d (a), P 2p (b) and W 4f (c) core level spectra of NbPW material. The binding energy scale was calibrated with respect to the C 1s peak.

the extraframework.[44] Notably, the peak at 320 nm blue-shifted to 302 nm for the NbPW-06 sample; this was likely not due to the quantum confinement effect because the sizes of the NbPW-06 samples were not comparable with their Bohr atomic radii.[45]

The TG analysis of the NbPW material is shown in Fig. S1.† The calcined catalysts showed no weight loss except the physically adsorbed water. Moreover, the TG analysis revealed that the niobium phosphotungstate exhibited high thermal stability. Furthermore, the high resolution XPS spectra of the niobium, phosphorus and tungsten in the NbPW material are shown in Fig. 4. The Nb 3d spectrum involves two characteristic peaks attributable to Nb $3d_{5/2}$ and Nb $3d_{3/2}$ at approximately 207.8 eV and 210.5 eV, respectively; this is characteristic of pentavalent niobium (Fig. 4(a)).[46] The peak located at a binding energy of 134.4 eV was associated with the phosphorous in P–OH species (Fig. 4(b)), and this peak confirmed the presence of P–OH groups on the surface of the prepared catalyst; the superficial enrichment of these groups appeared as an increased number of Brønsted acid sites.[47] The peaks at 35.7 eV and 37.8 eV were assigned to W $4f_{7/2}$ and W $4f_{5/2}$, at 35.7 eV and 37.8 eV were assigned to W $4f_{7/2}$ and W $4f_{5/2}$, respectively (Fig. 4(c)), indicating a blueshift in the binding energies compared with those of pure HPW;[48] the shift may be due to the interaction between the Keggin unit of the tungstophosphate anion $[PW_{12}O_{40}]^{3-}$ and the metal cation Nb^{5+}.

The SEM images confirmed that the NbPW was amorphous (Fig. S2†), whereas the TEM images of NbPW-06 revealed the presence of spherical particles (Fig. S3†). The compositional analysis of NbPW by X-ray fluorescence (XRF) and XPS is shown in Table 1. The phosphorus to niobium(v) molar ratios obtained from XRF analysis decreased gradually from 0.53 to 0.07 with increasing Nb content, and a similar trend was observed from the XPS analysis. However, there was significant difference between the total atomic composition and the surface atomic composition, indicating that the P species were superficially enriched when niobium atoms are incorporated into the framework of the catalysts. The P/W ratios determined from XRF did not vary consistently with increasing Nb content, and these values were much lower than those obtained from XPS analysis, indicating that the content of P species in the bulk phase decreased substantially. Therefore, the current synthetic method is suitable for enriching P species on the surface.

3.2 Acidity measurement

The number of total acid sites and acid strength of the catalysts were investigated by NH_3-TPD. The weak-, medium-, and strong-acid sites were measured according to their NH_3 desorption temperatures (150–300 °C, 300–500 °C, and 500–650 °C, respectively) (Fig. S4†). The concentrations of total acid sites on the calcined NbPW materials decreased with increasing Nb content (Table 1). As shown in Fig. S4 and S5,† the NH_3-TPD profiles of NbPW catalysts showed desorption peaks of weak-acid sites, which indicated the NbPW catalysts were weak-acid salts. In addition, there is a higher concentration of total acid sites on the as-synthesized NbPW-06 than on the calcined NbPW-06 (1.32 mmol g^{-1} and 0.89 mmol g^{-1}, respectively). The properties of the acid sites were monitored by using FTIR spectroscopy after pyridine chemisorption. As shown in Fig. 5, characteristic absorption bands at 1540 and 1635 cm^{-1}, corresponding to the Brønsted acid sites, were observed in the spectra of the NbPW samples.[49] The band at approximately 1445 cm^{-1}, consistent with pyridine molecules the adsorbed at the Lewis acid sites, was clear, whereas the corresponding bands in the spectra of NbPW-06 and NbPW-1 were very weak.[50,51] Additionally, a band at 1490 cm^{-1}, which could be attributed to the overlap of the Brønsted and Lewis acid sites, was also observed in the spectra of the catalysts.[52] The intensity of the band at 1540 cm^{-1} remained almost constant with increasing temperature, while the bands at 1445 cm^{-1} and 1490 cm^{-1} gradually decreased in intensity, indicating that the Brønsted acid sites are stronger than the Lewis acid sites (Fig. 5(a) and (b)). As seen in Table 1, all NbPW samples exhibited high Brønsted acidity, and a progressive decrease in the density of total Brønsted acid sites and a progressive increase in the density of total Lewis acid sites were observed increasing niobium loading, corresponding to the fact that Lewis acid sites were generated by the incorporated niobium species in the NbPW samples. The relative ratio of Brønsted and Lewis acid sites could be calculated by integrating the areas under the bands at 1540 cm^{-1} and 1455 cm^{-1}. The B/L ratio is mainly affected by the surface elements, and the more P species on the surface, the greater the Brønsted acid site ratio (Table 1). However, the content of P species in the bulk phase is much lower than that of the surface, suggesting that Brønsted acid sites originate from surface P species; more specifically, the sites likely originate from P–OH moieties, because P–OH groups can serve as sources of H, encouraging a spillover effect.[47] Therefore, NbPW-06 is characterized by a larger number of total Brønsted acid sites than the other synthesized compounds.

3.3 Effect of varying the composition of the catalyst on the selectivity of 5-HMF from fructose

The efficacies of catalysts with different compositions, metals, and heteropolyacids on the dehydration of fructose in DMSO were investigated at 80 °C using a reaction time of 3 h (Table 2). A small amount of 5-HMF was obtained using the blank

Table 1 Characterization of the NbPW by adsorption, pyridine FTIR, XRF and XPS studies

Catalyst	Density of total acid sites[a] (mmol g^{-1})	Density of Brønsted acid sites[b] (mmol g^{-1})	Density of Lewis acid sites[b] (mmol g^{-1})	B/L	P/Nb^{V} molar ratio[c]	P/W^{VI} molar ratio[c]	Surface atomic composition[d]				P/Nb^{V} molar ratio	P/W^{VI} molar ratio
							Nb	P	W	O		
NbPW-06	0.89	0.77	0.12	6.75	0.53	0.10	0.66	3.97	18.93	76.44	6.02	0.21
NbPW-1	0.74	0.54	0.20	2.74	0.43	0.12	1.44	4.03	25.23	69.3	2.80	0.16
NbPW-2	0.6	0.39	0.21	1.89	0.11	0.06	3.75	3.99	23.7	68.58	1.06	0.17
NbPW-4	0.48	0.25	0.23	1.09	0.07	0.09	7.03	4.6	20.33	68.04	0.65	0.22

[a] Determined from ammonia TPD. [b] Determined from pyridine- FTIR. [c] Determined by XRF. [d] Based on XPS analysis.

reference catalyst (Table 2, entry 1). When a heteropolyacid (Table 2, entry 2–4) was used, the yield of 5-HMF was relatively high, suggesting that H^{+} ions have a positive effect on the dehydration of fructose, which is consistent with the results reported by Xiao *et al.*[39] According to our results, a very similar yield of 5-HMF was obtained using either homogeneous $NbCl_5$ (Table 2, entry 5) or heterogeneous Nb_2O_5 (Table 2, entry 6) as the catalyst, indicating that Nb^{5+} could promote the conversion of fructose. Among the prepared NbPW catalysts, NbPW-06 (Table 2, entry 7) exhibited excellent catalytic activity in the dehydration of fructose and provided complete conversion of fructose and 96.7% yield of 5-HMF. As expected, as the Nb content increased, the yield of 5-HMF did not increase (Table 2, entry 8–10). The catalytic activity of NbPW-06 was higher than those of the other prepared catalysts, which was attributed to its higher acidity and appropriate content of Lewis and Brønsted acid sites required for the dehydration of fructose. In addition, the enhanced catalytic activity of NbPW-06 can be attributed to the presence of more Brønsted acid sites, and the yield of 5-HMF gradually increased with increasing total number of Brønsted acid sites. This confirmed the beneficial effect of Brønsted acidity for catalytic systems for the dehydration of fructose.

When using phosphomolybdic acid or HSiW as the raw material, the prepared NbSiW-08 (entry 12, Table 2) performed better than NbPMo-06 (entry 11, Table 2), but its catalytic activity was slightly lower than that of NbPW-06. Furthermore, all the phosphotungstate and silicotungstate species used in such reactions have exhibited better catalytic conversion results than that of phosphomolybdate.

Further investigations have been carried out by introducing various metal ions such as Sn^{4+}, Cr^{3+}, and Ce^{3+} (entry 13–15, Table 2). The use of SnPW-075 and CrPW-1 at 80 °C lead to 5-HMF yields of 76.5% and 81.5%, respectively, whereas a yield of 35.9% can be obtained using CePW-1 as a catalyst. These results suggest that the metal ions have a profound influence in the success of fructose dehydration, which can be attributed to the various metal ions playing different roles in the conversion of

Fig. 5 IR spectra of pyridine adsorbed on (a) NbPW-06 and (b) NbPW-1 after evacuation at (i) 100 °C, (ii) 150 °C and (iii) 200 °C. Absorbance peaks characteristic of Brønsted (B), Lewis (L), strong Lewis (SL) and weak Lewis (WL) sites are indicated.

Table 2 The results of fructose conversion after 3 h[a]

		As-synthesized			Calcined		
Entry	Catalyst	Fructose conv. (%)	5-HMF (%)	Selectivity (%)	Fructose conv. (%)	5-HMF (%)	Selectivity (%)
1	Blank	10.3	<0.5	<0.5	—	—	—
2	$H_3PW_{12}O_{40}$	99.7	83.6	83.9	—	—	—
3	$H_3PMo_{12}O_{40}$	70.4	46.1	65.5	—	—	—
4	$H_4SiW_{12}O_{40}$	99.3	86	86.6	—	—	—
5	$NbCl_5$	99.1	75.3	76	—	—	—
6	Nb_2O_5	99.5	73.7	74	—	—	—
7	NbPW-06	99.4	86.4	87	100	96.7	96.7
8	NbPW-1	99	78.8	79.6	98.7	89	90.1
9	NbPW-2	98.4	72.5	73.8	98.2	77.6	79
10	NbPW-4	98.1	67.3	68.6	97.2	73.4	75.5
11	NbPMo-06	75.8	41.3	54.5	70.6	32.7	46.3
12	NbSiW-08	99.5	81.6	82.1	98.3	79.4	80.7
13	SnPW-075	99.4	69.4	69.8	99.6	76.5	76.8
14	CrPW-1	99.6	76.8	77.2	99.7	81.5	81.7
15	CePW-1	64.5	32.1	49.8	59.3	35.9	60.5

[a] Conditions: 56 mM fructose, 50 mg catalyst, 80 °C, 5 mL DMSO, 3 h.

fructose. According to previous reports, Sn^{4+}, as a Lewis acidic ion, can interact with the fructose molecule, and this interaction and complex formation can promote the dehydration reaction.[53] Chromium atoms are the main contributors to the Lewis acidity of the catalyst, and the incorporation of Cr into the easily separable solid catalyst lessens the hazardous effects of Cr^{3+} and promote 5-HMF formation.[54,55] Moreover, Ce-based heteropolyacid salt catalysts have exhibited high catalytic activities in the conversion of fructose at higher temperatures. According to previous reports,[20,35,40] the NbPW catalyst showed more excellent catalytic activity under mild condition, indicating NbPW was a preferred catalyst with high efficiency of energy utilization, less pollution, lower energy consumption. Notably, the calcined material of each phosphotungstate catalyst tended to provide much higher yields of 5-HMF than the corresponding as-synthesized catalysts, which is in contrast with the results reported for phosphomolybdate and silicotungstate compounds.

The catalytic conversion of fructose to 5-HMF by NbPW within 6 min was studied (Table S1†). Conversions of fructose of approximately 50% were obtained, and the yields of 5-HMF gradually decreased with increasing Nb content in the catalyst. On one hand, the effect of the Nb loading was investigated by calculating the turnover frequencies (TOF based on total acid sites). On the other hand, the TOFs for each of the catalysts were different, suggesting that the observed changes in reactivity with various amounts of Nb could be attributed to a fundamental change in the reactivity of the available acid sites. NbPW-06 gave the highest TOF, and it was approximately 4.5 times higher than the TOF obtained in a previous study.[56] In addition, further decreases in the amount of incorporated Nb did not enhance the catalytic efficiency because the syntheses of catalysts with low Nb contents are lower yielding, making it difficult to produce heterogeneous catalyst with low Nb concentrations. Therefore, NbPW-06 can be considered the optimum catalyst as it provides the most suitable content of acid sites for the production of 5-HMF.

3.4 Effect of varying the solvent on the dehydration activity

First, the influence of different solvents on the fructose conversion was evaluated (Table 3). The yields and selectivities for 5-HMF varied remarkably in different solvents, suggesting the solvent effect was substantial. The high 5-HMF selectivity and yield in the fructose dehydration conducted DMSO have been explained (see Table 3, entry 1); DMSO can prevent the rehydration of 5-HMF to levulinic acid and formic acid and the formation of humins through the preferential coordination of DMSO to the 5-HMF, and DMSO can prevent fructose from undergoing reactions other than dehydration to 5-HMF through the specific coordination of DMSO to fructose.[57] In DMA, DMF, NMP, and acetone (see Table 3, entry 2–5) the conversions of fructose and the yields of 5-HMF were relatively high, which could be attributed to these polar aprotic solvents being well suited mediums for the reaction, effectively inhibiting side reactions, and easily solubilizing the reactants. With MIBK as the solvent (see Table 3, entry 6), NbPW-06 showed poor

Table 3 Conversion of fructose to 5-HMF with different solvents[a]

		Experimental parameter		
Entry	Solvent	Conversion/%	Yield/%	Selectivity/%
1	DMSO	100	96.7	96.7
2	DMA	87.1	31.3	35.9
3	DMF	91.8	33.5	36.5
4	NMP	96.7	70.3	72.8
5	Acetone	89.5	33.9	37.8
6	MIBK	91.5	1.3	1.5
7	*sec*-Butanol	92.8	26.3	28.3
8	*n*-Butanol	22.4	0.9	4.1
9	[EMIM]Br	50.6	5.3	10.5
10	H_2O	59.9	7.8	13.0
11	DMSO/H_2O (4 : 1)	82.9	5.9	7.2

[a] Conditions: 56 mM fructose, 50 mg NbPW-06, 80 °C, 3 h.

catalytic activity, and a large amount of humin was formed. Protic solvents, such as *sec*-butanol, facilitated the conversion of fructose; however, the yields and selectivities of 5-HMF were not high in these solvent (see Table 3, entry 7). These poor results may have been the result of side reactions in the *sec*-butanol. Moreover, the fructose dehydration was not efficient and the yield of 5-HMF was less than 10% in *n*-butanol, [EMIM]Br and water (see Table 3, entry 8–10) due to the formation of humins and rehydration of 5-HMF to levulinic acid and formic acid.[3] According to a previous report, the presence of water plays a key role in the dehydration of fructose when DMSO was as the solvent.[58] Nevertheless, the yield of 5-HMF was not as good as we expected because NbPW-06 showed poor catalytic activity in DMSO/H_2O (4 : 1 v/v). Briefly, DMSO was carefully chosen as the optimum solvent to obtain high yields of 5-HMF.

3.5 Effect of the processing conditions for the NbPW-06-catalyzed conversion of fructose to 5-HMF

In this study, the yields of 5-HMF in the NbPW material-catalyzed reactions were superior to those catalyzed by other heteropoly salts under mild conditions. Because NbPW-06 possesses a lower niobium content and is less expensive than other NbPW material, NbPW-06 was chosen for further focused studies on the conversion of fructose to 5-HMF.

Fig. 6(a) shows the influence of reaction temperature on the conversion of fructose to 5-HMF with NbPW-06 as the catalyst. Indeed, the fructose conversion and the 5-HMF yield were strongly influenced by the reaction temperature. As temperature increased, the rate of fructose conversion increased, and a high conversion of fructose (99%) was achieved within 20 min at 80 °C. At lower temperatures, the rate was substantially lower; for example, at 60 °C, a reaction time of 2 h was required to reach 98% fructose conversion. Obviously, lower yields of 5-HMF and slower reaction rates were obtained when the reaction temperature was below 80 °C. The yield of 5-HMF increased significantly when the reaction temperature was increased from 60 °C to 80 °C, and the highest 5-HMF yield (96.7%) was achieved at 80 °C. The higher the temperature reaction required the shortest reaction time to obtain the optimum yield. However, when the reaction temperature was above 80 °C, the yields of 5-HMF were lower than what was achieved at 80 °C, which could be attributed to the formation of a trace amounts of black humin oligomer. The color of the reaction solution also deepened at elevated temperature, although to a lesser extent than was observed at 60 °C. Therefore, 80 °C was the optimal temperature under these conditions.

Fig. 6(b) presents the effect of the initial fructose concentration on the fructose conversion and 5-HMF yield. Notably,

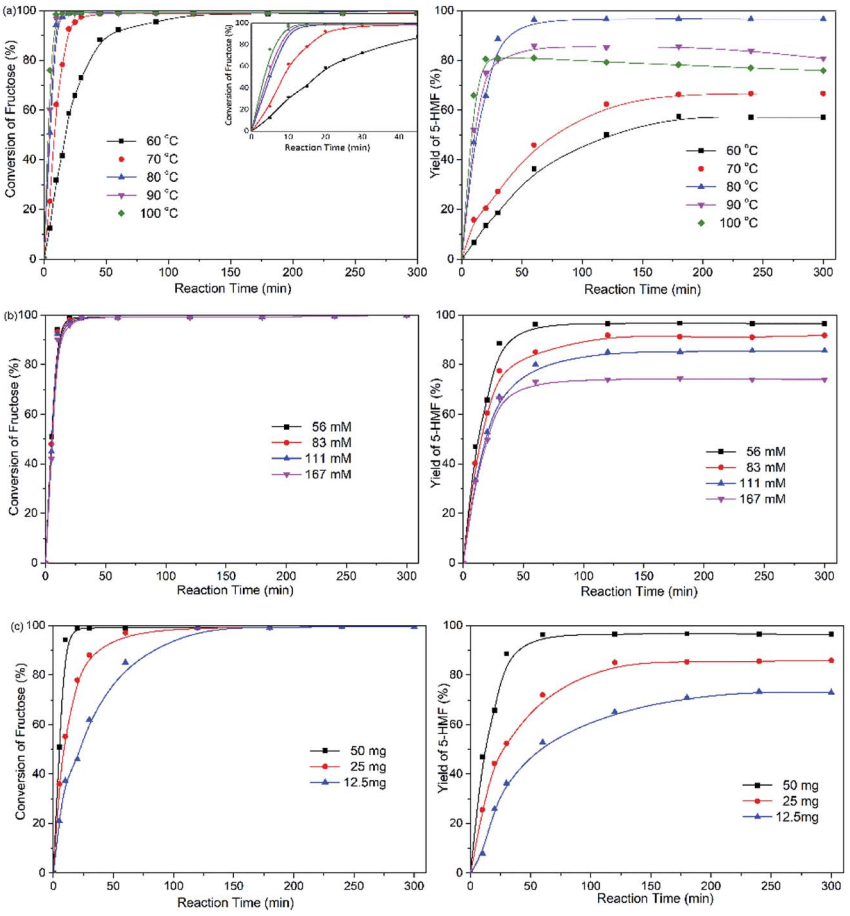

Fig. 6 Effect of (a) reaction temperature, (b) substrate concentration, and (c) catalyst loading on the conversion of fructose to 5-HMF (conditions: $[fructose]_o$ = 56 mM, NbPW-06 = 50 mg, 5 mL DMSO, 80 °C).

the fructose conversion was independent of the initial fructose concentration, suggesting that the dehydration of fructose was a first-order reaction with respect to fructose. However, the yield of 5-HMF was a function of the initial fructose concentration, and a lower initial concentration of fructose between 56 mM to 167 mM lead to a higher yield of 5-HMF. Low substrate concentrations tend to obtain high 5-HMF yields, which could be attributed that it was easier for the substrate molecules to diffuse in the solvent, thus accelerating the shift of reaction equilibrium to 5-HMF. When higher initial concentrations of fructose were employed, the reaction solution became deep yellow probably due to a side reaction.

The influence of the amount of NbPW-06 catalyst loading was investigated in the dehydration of fructose at 80 °C, and the results are shown in Fig. 6(c). Obviously, higher catalyst loading resulted in higher reaction rates, higher fructose conversion and higher 5-HMF yield. Fructose conversion and 5-HMF yield were maintained at 99% and 73%, respectively, when the catalyst loading was decreased to 12.5 mg. In addition, higher final yields of 5-HMF were detected with higher NbPW-06 concentrations; hence, 50 mg of catalyst was selected for obtaining high yields of 5-HMF.

3.6 Effect of calcination temperature on the catalytic activity of NbPW-06

To investigate the effect of calcination temperature on the catalytic activity of NbPW-06, NbPW-06 was calcined at different temperatures (100–600 °C) after treatment. The catalytic activities of the NbPW-06 samples calcined at varying temperatures are shown in Fig. 7(a). The NbPW-06 calcined at 100–500 °C exhibited an excellent performance in the conversion of fructose to 5-HMF with yields greater than 70% and selectivities greater than 90%. A calcination temperature of 300 °C is suitable for NbPW-06, which possessed high catalytic activity and achieved the highest yield and selectivity for 5-HMF. Desirable activity can be achieved with NbPW-06 material after calcination at 300 °C because of its appropriate acid strength and acid contents. In contrast, less than 5% yield of 5-HMF was obtained from fructose when NbPW-06 samples calcined at temperatures up to 600 °C were used, and this change might be caused by some deactivation on the surface of the catalyst due to the higher temperature; some distinct structural changes in these materials were suggested by the observed FTIR patterns (Fig. S6†).

3.7 Kinetic model

A kinetic analysis of the fructose conversion catalyzed by NbPW-06 in DMSO under mild conditions was performed, and the fructose conversion was identified as a first-order reaction.[12] The values of the pseudo-first-order rate constant (k) at different temperatures (T) were obtained by plotting $\ln(1 - x)$ *vs.* time (t) (where x is the conversion of fructose). The value of k increases gradually with increasing temperature, indicating that the fructose conversion is promoted by elevated reaction temperature (Table 4). Table 5 shows the kinetic parameters of the NbPW-06-catalyzed fructose conversion, and the apparent activation energy of the fructose conversion in this system was

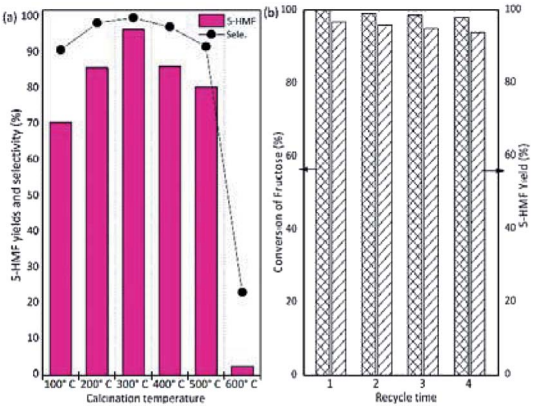

Fig. 7 (a) Effect of calcination temperature on the catalytic activity of NbPW-06; (b) reusability of NbPW-06 catalyst (conditions: $[\text{fructose}]_o$ = 56 mM, NbPW-06 = 50 mg, 5 mL DMSO, 80 °C).

54.09 kJ mol^{-1}, which is much lower than that reported by Moreau *et al.* (141 kJ mol^{-1}) when using zeolites as the catalyst.[59] The low activation energy of the NbPW-06-catalyzed system can minimize energy consumption and undesirable sugar degradation pathways,[60] allowing the dehydration of fructose to be conducted at moderate temperatures.

3.8 Catalyst recyclability

To study the long-term stability of the catalyst, four consecutive reactions were carried out with the NbPW materials. After the reaction, the NbPW catalyst was separated through centrifugation and recovered by washing and vacuum drying (120 °C), and the recovered catalyst was weighed to ensure a constant substrate-to-catalyst ratio (Fig. 7(b)). NbPW-06 was recycled four times without a significant decrease in the activity since a 94.0% yield of 5-HMF and a 98% fructose conversion were observed after four cycles. The slight decrease in the yield of 5-HMF can be attributed to the minor decrease in the activity of the NbPW materials or partial humins formation during the later reaction cycles. The somewhat higher weight-loss ratio of the recycled NbPW-06 (Table S2†) suggests a small amount of carbon deposition is occurring on the NbPW-06. The number of total acid sites decreased slightly during each cycle (Table S2†), demonstrating that the tungstophosphate anion $[PW_{12}O_{40}]^{3-}$ possessed excellent stability in DMSO. Thus, the NbPW-06 catalyst can be effectively separated and reused for the conversion of carbohydrates.

Table 4 Reaction rate constants (k) of fructose conversion at different reaction temperatures using NbPW-06[a]

Entry	Temp. (K)	k (min^{-1})	Correlation coefficient
1	333	0.0709	0.9909
2	343	0.1287	0.9935
3	353	0.2690	0.9833
4	363	0.3625	0.9855
5	373	0.5753	0.9941

[a] Conditions: 56 mM fructose, 50 mg NbPW-06, 5 mL DMSO, 5 min.

Table 5 Kinetic parameters of the fructose conversion using NbPW-06

Parameter	Value
Reaction order, n	1
Activation energy, E_a (kJ mol^{-1})	54.09
Pre-exponential factor, A (min^{-1})	2.3×10^6
Correlation coefficient	0.9864

3.9 Effect of various substrates on the dehydration activity

NbPW-06 is a solid catalyst with Brønsted acid sites that can catalyze this hydrolysis reaction, and it allows a tandem hydrolysis-dehydration pathway for converting disaccharides and polysaccharides into 5-HMF in a one-pot method. In addition, NbPW-06 is very active in the dehydration of sugars containing fructose units. Furthermore, when this catalytic system was applied to the dehydration of other substrates to 5-HMF, satisfactory yields were achieved from sucrose and inulin (Table 6). The conversion could reach over 95%, and the yield and selectivity were more than 50%, which indicated that NbPW-06 could play an important role in the hydrolysis and dehydration of disaccharides and polysaccharides.

3.10 Mechanism of 5-HMF formation in DMSO catalyzed by NbPW-06 under mild conditions

NbPW-06 showed excellent catalytic activity in our reaction system under mild conditions. To a certain degree, the role of niobium is to change the distribution of P species in the bulk phase and on the surface of the catalyst. The incorporation of Nb species during catalyst formulation enriches the P species on the surface of the catalyst. Brønsted acid sites originate from P species, and more specifically from P–OH groups, enriched on the surface of the catalyst. The proposed reaction mechanism for the conversion of fructose to 5-HMF is presented in Scheme 1. The first dehydration step from a cyclic D-fructose would yield the enol form of intermediate **2**, whose formation was the rate-limiting step. The hydrogen proton from P–OH on the surface of NbPW-06 could accelerate the first dehydration of D-fructose, and the protonation and deprotonation occur at different functional groups on D-fructose, so that the hydrogen proton on NbPW-06 could be at an equilibrium. This step is followed by two consecutive β-dehydrations in the ring to form the 5-HMF, which was observed to proceed slower than when starting from fructose. Generally, D-fructose lost three water molecules to 5-HMF through the gain and loss circulation of the hydrogen proton on the surface of the NbPW-06. There was no levulinic acid (LA) or formic acid (FA) detected under the optimal conditions; therefore, the proposed reaction pathway does not include the rehydration of 5-HMF to LA and FA. The 96.7% yield of 5-HMF from fructose confirmed that the Brønsted acid sites on NbPW-06 were sufficiently active to catalyze the dehydration under mild conditions. Scheme 2 presents the proposed reaction pathways for the conversion of fructose to 5-HMF over the NbPW-06 catalyst in DMSO including the dehydration of fructose to 5-HMF on the Brønsted acid sites. Additionally, no insoluble humins were observed, and the color of the reaction solution remained light yellow under mild conditions because the lower temperature minimized the side reactions and could not support the formation of the by-products. The rehydration of 5-HMF to LA and FA is prevented in this reaction system; hence, it allows 5-HMF to be produced directly from fructose with high selectivity.

Table 6 Catalytic conversion of various substrates to 5-HMF by NbPW-06[a]

		Experimental parameter		
Entry	Substrate	Conversion/%	Yield/%	Selectivity/%
1	Fructose	99.6	96.7	97.1
2	Sucrose	96.7	52.2	54.0
3	Inulin	98.2	53.3	54.3

[a] Conditions: 56 mM substrate, 50 mg NbPW-06, 5 mL DMSO, 80 °C, 3 h.

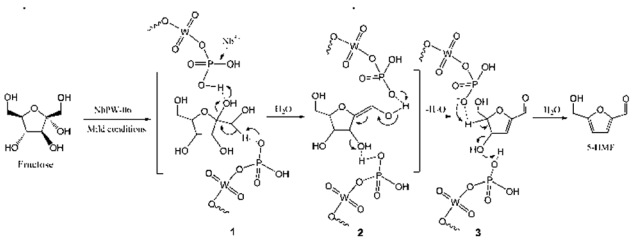

Scheme 1 Proposed reaction mechanism for the conversion of fructose to 5-HMF.

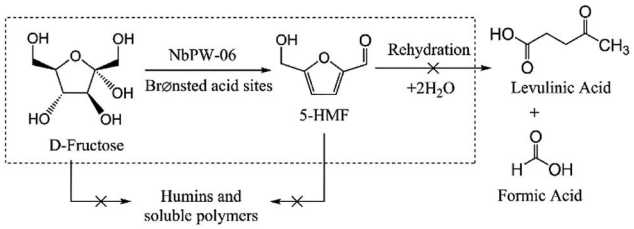

Scheme 2 Possible pathway for the conversion of fructose to 5-HMF in DMSO over NbPW-06 under mild condition.

4. Conclusions

This work offered a preliminary study on the feasibility of using NbPW materials as highly active catalysts for the conversion of fructose to 5-HMF under mild conditions. A high yield (96.7%) could be achieved from fructose in DMSO at 80 °C with a reaction time of 1.5 h. The loading of Nb impacted the activity of the NbPW catalyst, and NbPW-06 showed the best performance because it provided the optimum number of Brønsted acid sites for this dehydration reaction. The incorporation of Nb species changes the distribution of P species in the bulk phase and at the surface of the catalyst, and additional Nb promotes the enrichment of P–OH groups on the surface of the catalyst, which generates Brønsted acid sites that facilitate the production of 5-HMF. A possible reaction pathway involving the Nb-

compound as the catalyst was proposed. Moreover, a strategy that introduces the active component, Nb, into the heterogeneous catalysts could be applicable for the conversion of carbohydrates, which will make it an efficient and green method for the production of 5-HMF.

Conflicts of interest

There are no conflicts to declare.

Acknowledgements

This study was sponsored by the National Natural Science Foundation of China under grant number 21476021.

Notes and references

1 D. M. Alonso, S. G. Wettstein and J. A. Dumesic, *Green Chem.*, 2013, **15**, 584–595.
2 X. Wang, F. Liang, C. Huang, Y. Li and B. Chen, *Catal. Sci. Technol.*, 2015, **5**, 4410–4421.
3 R.-J. van Putten, J. C. van der Waal, E. de Jong, C. B. Rasrendra, H. J. Heeres and J. G. de Vries, *Chem. Rev.*, 2013, **113**, 1499–1597.
4 C. Chatterjee, F. Pong and A. Sen, *Green Chem.*, 2014, **17**, 40–71.
5 M. Besson, P. Gallezot and C. Pinel, *Chem. Rev.*, 2014, **114**, 1827–1870.
6 C. Li, X. Zhao, A. Wang, G. W. Huber and T. Zhang, *Chem. Rev.*, 2015, **115**, 11559.
7 M. E. Zakrzewska, E. Bogel-Łukasik and R. Bogel-Łukasik, *Chem. Rev.*, 2011, **111**, 397–417.
8 H. Tang, N. Li, F. Chen, G. Li, A. Wang, Y. Cong, X. Wang and T. Zhang, *Green Chem.*, 2017, **19**, 1855–1860.
9 J. J. Roylance and K. S. Choi, *Green Chem.*, 2016, **18**, 2956–2960.
10 X. Kong, R. Zheng, Y. Zhu, G. Ding, Y. Zhu and Y. W. Li, *Green Chem.*, 2015, **17**, 2504–2514.
11 Z. Xue, B. Cao, W. Zhao, J. Wang, T. Yu and T. Mu, *RSC Adv.*, 2016, **6**, 64338–64343.
12 M. Bicker, J. Hirth and H. Vogel, *Green Chem.*, 2003, **5**, 280–284.
13 F. S. Asghari and H. Yoshida, *Ind. Eng. Chem. Res.*, 2013, **46**, 7703–7710.
14 J. B. Binder and R. T. Raines, *J. Am. Chem. Soc.*, 2009, **131**, 1979–1985.
15 S. Yue, J. Sun, Y. Yi, W. Bo, X. Feng and R. Sun, *J. Mol. Catal. A: Chem.*, 2014, **394**, 114–120.
16 J. Liu, Y. Tang, K. Wu, C. Bi and Q. Cui, *Carbohydr. Res.*, 2012, **350**, 20–24.
17 S. Siankevich, Z. Fei, R. Scopelliti, G. Laurenczy, S. Katsyuba, N. Yan and P. J. Dyson, *Chemsuschem*, 2014, **7**, 1647.
18 A. H. Jadhav, H. Kim and I. T. Hwang, *Catal. Commun.*, 2012, **21**, 96–103.
19 Y. Ma, S. Qing, L. Wang, N. Islam, S. Guan, Z. Gao, X. Mamat, H. Li, W. Eli and T. Wang, *RSC Adv.*, 2015, **5**, 47377–47383.
20 Q. Zhao, L. Wang, S. Zhao, X. Wang and S. Wang, *Fuel*, 2011, **90**, 2289–2293.
21 X. Qi, H. Guo and L. Li, *Ind. Eng. Chem. Res.*, 2011, **50**, 7985–7989.
22 Z.-Z. Yang, J. Deng, T. Pan, Q.-X. Guo and Y. Fu, *Green Chem.*, 2012, **14**, 2986–2989.
23 R. Kourieh, V. Rakic, S. Bennici and A. Auroux, *Catal. Commun.*, 2013, **30**, 5–13.
24 H. M. Xu, Z. C. Miao, H. H. Zhao, J. Yang, J. Zhao, H. L. Song, N. Liang and L. J. Chou, *Fuel*, 2015, **145**, 234–240.
25 G. Sampath and S. Kannan, *Catal. Commun.*, 2013, **37**, 41–44.
26 F. H. Richter, K. Pupovac, R. Palkovits and F. Schüth, *ACS Catal.*, 2016, **3**, 123–127.
27 E. Nikolla, Y. RománLeshkov, M. Moliner and M. E. Davis, *ACS Catal.*, 2011, **1**, 408–410.
28 Z. G. Hu, Y. W. Peng, Y. J. Gao, Y. H. Qian, S. M. Ying, D. Q. Yuan, S. Horike, N. Ogiwara, R. Babarao, Y. X. Wang, N. Yan and D. Zhao, *Chem. Mater.*, 2016, **28**, 2659–2667.
29 Y. Peng, Z. Hu, Y. Gao, D. Yuan, Z. Kang, Y. Qian, N. Yan and D. Zhao, *Chemsuschem*, 2015, **8**, 3208–3212.
30 N. T. do Prado, T. E. Souza, A. R. T. Machado, P. P. Souza, R. S. Monteiro and L. C. A. Oliveira, *J. Mol. Catal. A: Chem.*, 2016, **422**, 23–34.
31 Y. Zhang, J. Wang, J. Ren, X. Liu, X. Li, Y. Xia, G. Lu and Y. Wang, *Catal. Sci. Technol.*, 2012, **2**, 2485–2491.
32 P. Carniti, A. Gervasini, F. Bossola and V. D. Santo, *Appl. Catal., B*, 2016, **193**, 93–102.
33 F. Wang, H. Z. Wu, C. L. Liu, R. Z. Yang and W. S. Dong, *Carbohydr. Res.*, 2013, **368**, 78–83.
34 E. L. S. Ngee, Y. Gao, X. Chen, T. M. Lee, Z. Hu, D. Zhao and N. Yan, *Ind. Eng. Chem. Res.*, 2014, **53**, 14225–14233.
35 F. N. D. C. Gomes, F. M. T. Mendes and M. M. V. M. Souza, *Catal. Today*, 2017, **279**(part 2), 296–304.
36 X. Zhang, D. Zhang, Z. Sun, L. Xue, X. Wang and Z. Jiang, *Appl. Catal., B*, 2016, **196**, 50–56.
37 B. Zhang, H. Asakura and N. Yan, *Ind. Eng. Chem. Res.*, 2017, **56**, 3578–3587.
38 B. Zhang, H. Asakura, J. Zhang, J. Zhang, S. De and N. Yan, *Angew. Chem., Int. Ed.*, 2016, **55**, 8319–8323.
39 Y. P. Xiao and Y. F. Song, *Appl. Catal., A*, 2014, **484**, 74–78.
40 C. Fan, H. Guan, Z. Hang, J. Wang, S. Wang and X. Wang, *Biomass Bioenergy*, 2011, **35**, 2659–2665.
41 S. Wang, Z. Zhang, B. Liu and J. Li, *Catal. Sci. Technol.*, 2013, **3**, 2104–2112.
42 I. V. Kozhevnikov, K. R. Kloetstra, A. Sinnema, H. W. Zandbergen and H. V. Bekkum, *J. Mol. Catal. A: Chem.*, 1996, **114**, 287–298.
43 Y. Sun, P. Afanasiev, M. Vrinat and G. Coudurier, *J. Mater. Chem.*, 2000, **10**, 2320–2324.
44 K. M. Parida, S. Rana, S. Mallick and D. Rath, *J. Colloid Interface Sci.*, 2010, **350**, 132–139.
45 A. N. Mallika, A. R. Reddy and K. V. Reddy, *J. Mater. Sci.: Mater. Electron.*, 2016, **27**, 1528–1534.
46 Z. Xue, Y. Zhang, G. Li, J. Wang, W. Zhao and T. Mu, *Catal. Sci. Technol.*, 2016, **6**, 1070–1076.

47 E. Rodríguez-Aguado, A. Infantes-Molina, D. Ballesteros-Plata, J. A. Cecilia, I. Barroso-Martín and E. Rodríguez-Castellón, *J. Mol. Catal.*, 2017, **437**, 130–139.
48 X. Kong, S. Wu, L. Liu, S. Li and J. Liu, *J. Mol. Catal.*, 2017, **439**, 180–185.
49 R. M. West, M. S. Holm, S. Saravanamurugan, J. Xiong, Z. Beversdorf, E. Taarning and C. H. Christensen, *J. Catal.*, 2010, **269**, 122–130.
50 S. K. Das, M. K. Bhunia, A. K. Sinha and A. Bhaumik, *ACS Catal.*, 2011, **1**, 493–501.
51 C. F. De, M. Dusselier, R. R. Van, P. Vanelderen, J. Dijkmans, E. Makshina, L. Giebeler, S. Oswald, G. V. Baron and J. F. Denayer, *J. Am. Chem. Soc.*, 2012, **134**, 10089.
52 M. G. Mazzotta, D. Gupta, B. Saha, A. K. Patra, A. Bhaumik and M. M. Abu-Omar, *Chemsuschem*, 2014, **7**, 2342.
53 Y. Qiao, C. M. Pedersen, D. Huang, W. Ge, M. Wu, C. Chen, S. Jia, Y. Wang and X. Hou, *ACS Sustainable Chem. Eng.*, 2016, **4**, 3327–3333.
54 X. Yi, I. Delidovich, Z. Sun, S. Wang, X. Wang and R. Palkovits, *Catal. Sci. Technol.*, 2015, **5**, 2496–2502.
55 H. Zhao, J. E. Holladay, H. Brown and Z. C. Zhang, *Science*, 2007, **316**, 1597.
56 J. M. R. Gallo, R. Alamillo and J. A. Dumesic, *J. Mol. Catal. A: Chem.*, 2016, **422**, 13–17.
57 S. H. Mushrif, S. Caratzoulas and D. G. Vlachos, *Phys. Chem. Chem. Phys.*, 2012, **14**, 2637–2644.
58 M. Zhang, X. Tong, R. Ma and Y. Li, *Catal. Today*, 2016, **264**, 131–135.
59 C. Moreau, R. Durand, S. Razigade, J. Duhamet, P. Faugeras, P. Rivalier, P. Ros and G. Avignon, *Appl. Catal., A*, 1996, **145**, 211–224.
60 X. Wang, Y. Song, C. Huang, F. Liang and B. Chen, *Green Chem.*, 2014, **16**, 4234–4240.